Articles

The widespread regulatory role of the phosphorylation of RNA-binding proteins (RBPs) in RNA abnormalities

DOI:https://dx.doi.org/10.71373/a1wrp114
Submitted 19 January 2026
Accepted 21 April 2026
Published 24 April 2026

Ziyi Liu[1#], Jinwan Li[1], Ping Cui[1*], Sanqi An[1,2*], Jing Leng[2,3*]

Protein phosphorylation is a pervasive post-translational modification that orchestrates cellular signal transduction and functional control during tumorigenesis. By charting a pan-cancer phosphoproteomic atlas with a focus on RNA-binding proteins (RBPs), we found that differentially phosphorylated sites between tumors and matched non-tumor tissues are strongly enriched on RBPs. These data suggest that phosphorylation can amplify oncogenic signals through RBP-mediated RNA dysregulation. Among all RBPs, phosphorylation of Nucleolin (NCL) at threonine 76 (NCL T76) is upregulated across multiple cancer types and is tightly associated with poor patient prognosis and widespread abnormalities in RNA processing. We systematically mapped the upstream kinase–substrate landscape and actionable compounds for this key RBP phosphosite and the downstream classes of RNA dysregulation linked to these modifications. Integrative analyses and in vitro experiments identify cyclin-dependent kinase 2 (CDK2) as the upstream kinase for NCL T76. The small molecule inhibitor TG-02 effectively suppresses CDK2-mediated phosphorylation at NCL T76. Our study establishes RBP phosphorylation as a prevalent regulatory layer across cancers that reshapes RNA regulatory networks. It further defines NCL T76 as a critical functional site, elucidates its upstream control, and highlights the CDK2–NCL T76 axis as a tractable therapeutic avenue.

Introduction

In the central dogma of molecular biology, the core role of RNA is to serve as a messenger directing protein synthesis. However, current research has revealed that the relationship between RNA and proteins is a profound, bidirectional dynamic regulation. Proteins, in turn, exert comprehensive and precise control over the entire lifecycle of RNA—from transcription and processing to degradation—among which protein phosphorylation stands as a key regulatory mechanism. The imbalance in this bidirectional interaction is closely linked to cancer development. Once this regulatory circuit becomes dysfunctional, it can directly drive the malignant progression of tumors.

RNA-binding proteins (RBPs) refer to a group of proteins capable of binding to single- or double-stranded RNA to form ribonucleoprotein complexes[1]. Through advanced high-throughput screening technologies and validation across multiple cell types, approximately 2,000 *Homo sapiens* RBPs (accounting for 7.5% of protein-coding genes) have been identified. These RBPs interact with RNA via RNA-binding domains and exert critical regulatory functions in gene expression at the transcriptional, post-transcriptional, and translational stages. They affect RNA splicing, stability, polyadenylation, localization, and translation during the RNA life cycle, resulting in abnormal protein phenotypes[2]. Increasing evidence indicates that their dysregulation or dysfunction can lead to various human diseases, including cancer. Research has also shown that the function of RBPs is dynamically regulated by post-translational modifications such as phosphorylation. Phosphorylation can notably affect the RNA binding affinity, subcellular localization, and stress granule formation of RBPs, thereby regulating processes such as alternative splicing, spliceosome assembly, and selective exon inclusion[3]. Nevertheless, how does RBP phosphorylation regulate a diverse spectrum of cancer characteristics by reshaping the intermediate layer of RNA modifications? Currently, there remains a substantial knowledge gap in systematic research on this regulatory axis, particularly in pan-cancer.

In this study, we systematically analyzed phosphorylation abnormalities of RNA-binding proteins (RBPs) using integrated phosphoproteomic and proteomic datasets across pan-cancer cohorts. Key differential phosphorylation sites on RBPs were identified, revealing that RBP phosphorylation represents an important yet largely overlooked molecular feature in cancer. Clinical correlation analyses further demonstrated the strong clinical significance of RBP phosphorylation[4]. We selected one representative RBP for experimental validation and predicted its upstream regulatory kinases and potential small-molecule inhibitors, which were subsequently verified through cellular assays. Collectively, these findings highlight the broad importance of RBP phosphorylation in cancer development and progression and underscore its potential for identifying novel therapeutic targets[5].

Materials and Methods

Data acquisition and preprocessing

The proteomic and phosphoproteomic data used in this study were obtained from the CPTAC database (https://proteomic.datacommons.cancer.gov/pdc/), including breast cancer (BRCA), glioblastoma (GBM), clear cell renal cell carcinoma (CCRCC), colon adenocarcinoma (COAD), head and neck squamous cell carcinoma (HNSCC), lung squamous cell carcinoma (LSCC), lung adenocarcinoma (LUAD), ovarian cancer (OV), pancreatic ductal adenocarcinoma (PDAC), and endometrial cancer (UCEC). The phosphorylation data were uniformly represented by the normalized intensity value after log2 transformation. To

1 Life Sciences Institute, Biosafety Level-3 Laboratory, Guangxi Medical University, Nanning 530021, China.
2 School of Basic Medical Sciences, Department of Biochemistry and Molecular Biology, Guangxi Medical University, Nanning 530021, China.
3 Department of Immunology, Guangxi Medical University, Nanning, Guangxi 530021, China.
#Equal contribution
**Corresponding author:*
Sanqi An (ansanqi@sr.gxmu.edu.cn)
Jing Leng (lj986771558@163.com)

ensure data quality, samples and phosphorylation sites with an excessively high proportion of missing values were removed, and the remaining missing values were imputed using row means. The signal intensity of phosphorylated proteins was divided by that of their corresponding total proteins to correct for differences in sample loading and to reflect the true phosphorylation state.

Differential phosphorylation analysis

In this study, the limma package in R software was employed to conduct differential phosphorylation analysis on the normalized data, aiming to identify differential phosphorylation sites between tumor and normal samples. The threshold was set at FDR < 0.05. The analytical method operates within a linear model framework, optimizing standard errors through an empirical Bayes shrinkage algorithm to compute adjusted t-statistics and their corresponding *p*-values. By integrating variation information from all phosphorylation sites in the dataset, this approach significantly enhances the robustness and testing power of statistical inference under small sample conditions.

Enrichment analysis

Gene Ontology (GO) analysis was performed on the differentially phosphorylated gene sites using the clusterProfiler R package, which can directly retrieve and integrate official annotation information from the GO database through its built-in interface. To mitigate the risk of false positives caused by multiple hypothesis testing, the Benjamini-Hochberg method was applied to adjust the *p*-values from the enrichment analysis, with a corrected false discovery rate (FDR) < 0.01 as the significance threshold. The significantly enriched GO-MF terms were selected and visualized in a heatmap.

Intersection analysis

Intersection analysis was performed on the significantly differential protein phosphorylation sites of various cancers, and an Upset plot was generated using the Upset Plot module of TBtools software. The results display the intersection of differential protein phosphorylation sites and their kinases in at least 4 types of cancers.

Correlation analysis

The visualization of correlation analysis was performed using the ggplot2 and ggpubr packages in R. Scatter plots were generated with phosphorylation levels as the x-axis and RNA pathway scores along with patient clinical information scores as the y-axis. The geom_smooth function was employed to add a blue fitted curve based on a linear regression model (method = "lm"), displaying the default 95% confidence interval (se = TRUE). The Pearson correlation coefficient and its statistical significance were automatically calculated and annotated by the stat_cor function.

Kinase prediction

To obtain the potential kinases corresponding to the previously screened phosphorylation site, the 15-amino-acid sequence surrounding this site (centered on the site, with 7 amino acids extended upstream and downstream) was submitted to the PhosphoSitePlus website (https://www.phosphosite.org/). A Sankey diagram of the phosphorylation sites and their regulatory kinases was plotted across pan-cancer.

Molecular docking

Based on the crystal structure of the key kinase identified, virtual screening of the HY-L001 bioactive compound library from MedChemExpress was performed using AutoDock Vina. By systematically evaluating the binding affinity and interaction patterns between small molecules and the kinase domain, molecular docking was conducted with the top 20 candidate molecules exhibiting optimal binding energy using AutoDock software. Suitable small molecules were selected for subsequent studies based on binding energy and chemical bond interactions.

Cell culture

The human pancreatic carcinoma cell line PANC-1 was purchased from the Cell Bank of the Committee on Type Culture Collection of the Chinese Academy of Sciences (National Collection of Authenticated Cell Cultures). The cells were cultured in high-glucose Dulbecco's Modified Eagle Medium (DMEM, Gibco, USA), supplemented with 10% fetal bovine serum (FBS, Gibco, USA) and 1% penicillin-streptomycin antibiotic mixture (Penicillin-Streptomycin Solution, Gibco, USA). The cells were maintained in a constant-temperature incubator at 37°C with 5% CO_2 and saturated humidity.

Small molecule inhibitor kinase assay

To investigate the effect of the CDK2 inhibitor on cellular phosphorylation levels, the cells were randomly divided into three groups: the control group received only an equal volume of dimethyl sulfoxide (DMSO, Sigma-Aldrich, USA); the two experimental groups were treated with the CDK2-specific inhibitor CDK2-IN-23（TG-02） (MedChemExpress, USA), achieving final concentrations of 0.5 μM and 1 μM, respectively. When the density of PANC-1 cells reached 50-60%, dimethyl sulfoxide (control group) and CDK2-IN-23（TG-02）(treatment group) were added, followed by continued culture for 24 hours for subsequent protein extraction and phosphorylation analysis.

Western Blotting

Total proteins were extracted from cells using RIPA lysis buffer, and protein concentration was determined by the BCA method. Samples were denatured at 100°C for 10 min, and 40 μg of protein was loaded per lane for electrophoresis. After electrophoresis, proteins were transferred onto a 0.2 μm PVDF membrane. The membrane was blocked with 5% skim milk blocking buffer. Primary antibodies (Anti-Nucleolin (phospho T76) antibody, Abcam, ab168363; Anti-Nucleolin antibody, Abcam, ab129200; Anti-beta Actin antibody, Abcam, ab6276) were added and incubated overnight at 4°C on a shaker. The PVDF membrane was then incubated with secondary antibodies (Goat Anti-Mouse IgG H&L (HRP), Abcam, ab6789; Goat Anti-Rabbit IgG H&L (HRP), Abcam, ab6721) at 37°C for 60 min on a shaker. ECL chemiluminescent substrate was used for reaction, and images were developed and captured using the Tanon 5200 gel imaging system.

Results

Phosphoproteomic landscape reveals widespread RBP phosphorylation abnormalities in pan-cancer

The phosphoproteomic and proteomic data from the CPTAC database were collected to screen for differential phosphorylation sites in tumor tissues compared to normal tissues, including endometrial cancer (UCEC), clear cell renal cell carcinoma (CCRCC), colon adenocarcinoma (COAD), head and neck squamous cell carcinoma (HNSCC), lung squamous cell carcinoma (LSCC), lung adenocarcinoma (LUAD), ovarian cancer (OV), and pancreatic adenocarcinoma (PDAC). Differential phosphorylation between tumor and normal tissues was analyzed for these tumor types (Figure 1A). Breast invasive carcinoma (BRCA) and glioblastoma multiforme (GBM) were excluded from this analysis due to the absence of normal tissue data[6]. The results revealed that in CCRCC, there were 4,102 RBP phosphorylation sites that were upregulated and 5,167 that were downregulated; in COAD, 72 upregulated and 39 downregulated; in HNSCC, 5,898 and 5,350; in LSCC, 8,206 and 6,942; in LUAD, 7,496 and 5,454; in OV, 1,796 and 1,181; in PDAC, 5,647 and 5,410; and in UCEC, 4,190 and 3,221, respectively (Figure 1A). These results indicate that widespread protein phosphorylation exists across all eight tumor types, confirming the significant role of protein phosphorylation modifications in cancer development[7]. Subsequently, GO enrichment was performed on the aberrant protein phosphorylation sites in the eight cancer types using DAVID, and it was revealed that these differentially phosphorylated sites were primarily enriched in protein binding and RNA binding (Figure 1B). This finding underscores the role of RNA regulation in the tumors with aberrant phosphorylation, further suggesting that protein phosphorylation may contribute to cancer progression by influencing RNA regulatory processes[8].

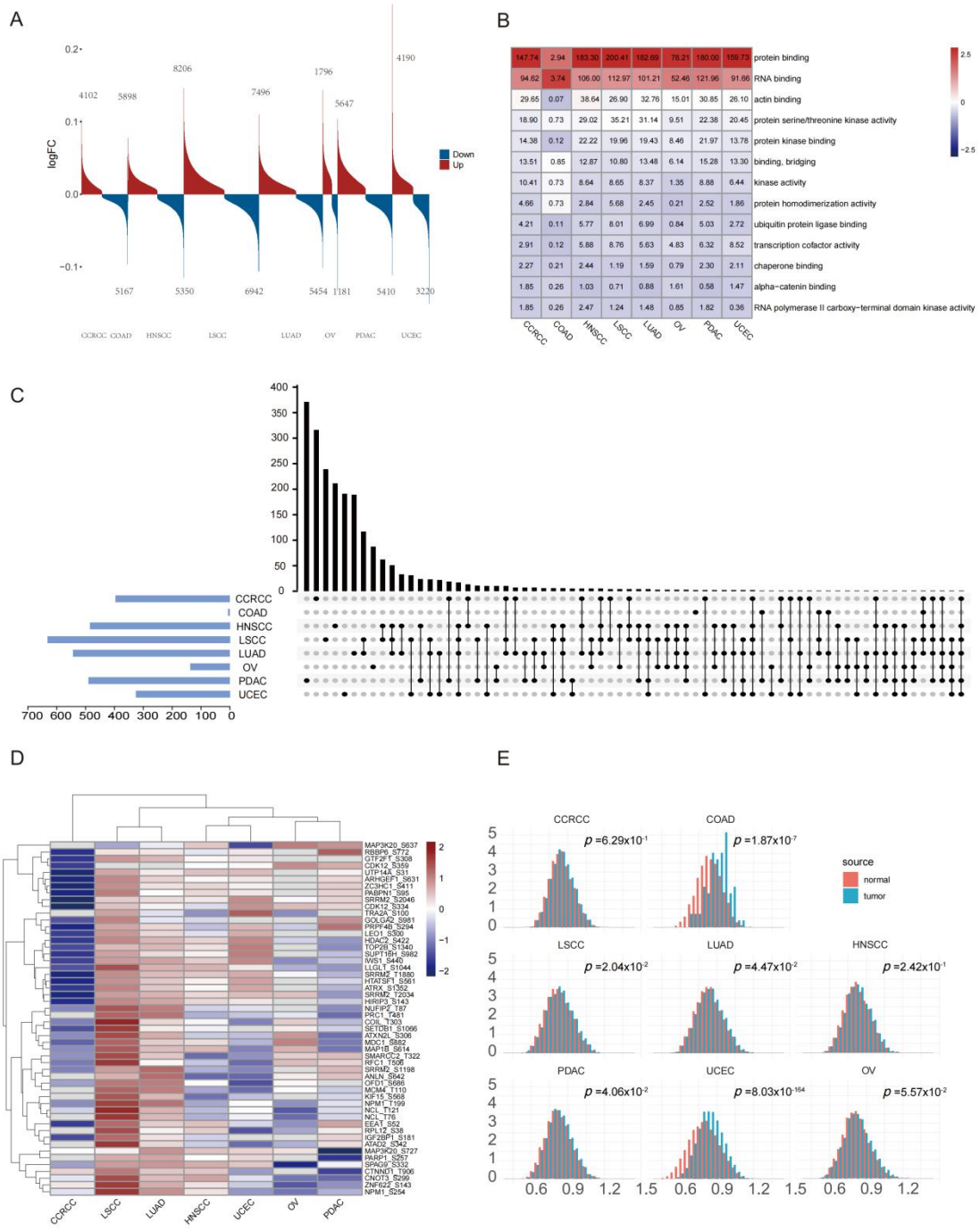

Figure 1.Comprehensive profiles of global protein phosphorylation and RBP phosphorylation in diverse cancer types. (A) The gene sites that exhibit upregulated or downregulated phosphorylation in diverse cancer tissues when compared to normal tissues (p <0.01). The horizontal axis represents gene sites with altered phosphorylation in each tumor, while the vertical axis indicates the logarithmic value of the fold change (log2FC) in phosphorylation between tumor and normal tissues, with the positive values denoting upregulation (shown in red) and negative values downregulation (shown in blue). The criteria for defining differentially phosphorylated proteins are a false discovery rate (FDR) <0.01 and a fold change (FC) >1.1 or <0.91, ensuring the statistical significance and biological relevance of the screening results. (B) GO enrichment on the differentially phosphorylated gene loci in each type of cancer (p <0.01). (C) Intersection analysis on the top 10% of gene loci with upregulated RBP phosphorylation (log2FC) across various cancers (p <0.01). (D) Phosphorylation levels of the 52 RBP upregulated in at least four cancers identified through intersection analysis were subjected to cluster analysis. The color gradient represents the degree of the fold change. (E) The distribution histogram of phosphorylation levels was plotted at RBP gene loci for each type of cancer and normal group, and inter-group difference test was performed. The horizontal axis represents phosphorylation levels, while the vertical axis indicates the number of phosphorylation sites at each level.

RNA-binding proteins (RBPs) are the core executors of RNA biology, and their dysfunction is associated with the occurrence and development of various cancers[9]. The gene loci with upregulated RBP phosphorylation were ranked according to the degree of upregulation (log2FC). The top 10% of genes included 396 in CCRCC, 6 in COAD (due to limited original data), 485 in HNSCC, 632 in LSCC, 543 in LUAD, 137 in OV, 490 in PDAC, and 326 in UCEC. Using TBtools, an intersection analysis was performed on these upregulated genes, and the results revealed that 52 genes were significantly upregulated in 4 cancer types, 14 genes in 5 types, and 1 gene in 6 types (Figure **1**C). This demonstrates that these genes with upregulated RBP phosphorylation exhibit conservation across multiple cancers[10].

Among the 52 RBP gene loci identified by intersection analysis as being upregulated in at least four cancer types, a clustering analysis of their phosphorylation levels across eight cancer types revealed that, except for CCRCC, where the majority were downregulated, these 52 gene loci were generally upregulated in most tumors[11]. Notably, in LSCC and LUAD, over 90% of the gene loci showed a significant upregulation of phosphorylation (Figure **1**D). This demonstrates that the phosphorylation of these key RBPs is indeed elevated in most tumors and exhibits tumor-type-specific characteristics.

For each cancer type, a distribution histogram of RBP phosphorylation was generated for tumor and normal tissues, and between-group difference tests were performed[12]. The results revealed that RBP phosphorylation was generally higher in tumor tissues than in normal tissues across various cancers (Figure **1**E), indicating that upregulated RBP phosphorylation may be positively correlated with tumorigenesis and tumor development. This suggests that elevated RBP phosphorylation could serve as an activating factor in the occurrence and progression of tumors[13].

Expression characteristics of key RBP phosphorylation sites and their clinical relevance

Four RBP phosphorylation sites were selected from among the 52 key sites upregulated in at least four tumor types for subsequent studies based on their high upregulation magnitude, consistent upregulation across multiple cancer types, prognostic relevance, and the commercial availability of validated molecular tools: IGF2BP1_S181, SRRM2_T1880, TRA2A_S100, and NCL_T76.The phosphorylation of IGF2BP1 at S181 was upregulated in HNSCC, LSCC, LUAD, and PDAC, while those of SRRM2_T1880, TRA2A_S100, and NCL_T76 were significantly upregulated in HNSCC, LSCC, LUAD, and UCEC (Figure **1**C). Patient samples from different cancer types were ranked based on RBP phosphorylation. Subsequently, we assessed whether clinical characteristics of tumor patients (such as age, body mass index (BMI), tumor size, gender, stage, etc.) followed the same pattern of change as the phosphorylation levels of each RBP (Figure **2**A-C).

The results revealed that elevated phosphorylation of IGF2BP1 at S181 was accompanied by reduced progression-free survival (PFS_days) in LUAD and showed consistent correlations with tumor stage, necrosis features, mRNA deadenylation, and microRNA signature levels across multiple cancer types (Figure **2**A). Likewise, increased phosphorylation of SRRM2 at T1880 coincided with decreased PFS_days in LSCC and LUAD, as well as reduced overall survival (OS_days) in LSCC, and exhibited a potential correlation with tumor stage and RNA-related molecular features (Figure **2**B). Moreover, phosphorylation of TRA2A was positively associated with tumor-related mRNA deadenylation, and phosphorylation of TRA2A at S100 even exhibited a notable correlation with body mass index (BMI) (Figure **2**C).

NCL_T76 phosphorylation is associated with the prognosis of various tumors and their RNA regulation

Among the four candidate phosphorylation sites identified above(IGF2BP1_S181, SRRM2_T1880, TRA2A_S100, and NCL_T76), NCL_T76 was prioritized for subsequent experimental validation based on two considerations. First, this site is extensively involved in RNA regulatory pathways across multiple cancer types (as shown below). Second, well-validated molecular tools for this site are commercially available. The clinical relevance of the other three sites (IGF2BP1_S181, SRRM2_T1880, and TRA2A_S100) was confirmed by bioinformatic analysis (Figure **3**A-C). However, detailed functional investigation of these three sites is beyond the scope of the current study and will be pursued in future work.

The pan-cancer overview in the waterfall plot revealed the association between known molecular and clinical features and NCL_T76 phosphorylation (Figure **3**A). As described above, NCL_T76 expression was elevated in HNSCC, LSCC, LUAD, OV, PDAC, and UCEC (Figure **1**C). Further correlation analyses revealed that the phosphorylation level of NCL_T76 was significantly negatively correlated with PFS_days and OS_days in certain cancer types (Figure **3**B-D). In OV, LUAD, and PDAC, NCL_T76 phosphorylation was significantly negatively correlated with OS_days (Figure **3**B,D). These findings suggest that elevated phosphorylation at the NCL_T76 site may serve as an independent risk factor for poor prognosis in LUAD, PDAC,

and OV.

To investigate the relationship between RBP phosphorylation and molecular features in tumors, we further analyzed the correlation between phosphorylation at NCL_T76 and RNA-related as well as cancer-related pathways[14]. In HNSCC, LUAD, PDAC, and UCEC, NCL_T76 phosphorylation exhibited a significant negative correlation with PD-1/PD-L1 expression (Figure 3E). In LSCC, LUAD, PDAC, and UCEC, elevated NCL_T76 phosphorylation showed a significant correlation with "tRNA modification in the mitochondrion," an important RNA modification pathway whose downregulation is closely associated with tumorigenesis (Figure 3F). In HNSCC, LSCC, LUAD, and UCEC, phosphorylation at NCL_T76 was negatively correlated with "Choline metabolism in cancer," indicating that elevated phosphorylation is associated with suppressed choline metabolism (Figure 3G). Furthermore, in LSCC, HNSCC, and UCEC, NCL_T76 phosphorylation was significantly positively correlated with "mRNA Splicing" (Figure3H). Additionally, in PDAC and LUAD, the phosphorylation level at this site was also correlated with "rRNA modification" (Figure 3I). In HNSCC, LUAD, and PDAC, NCL_T76 phosphorylation displayed a significant positive correlation with "Transcriptional misregulation in cancer," suggesting that increased phosphorylation at this site may promote transcriptional dysregulation and cancer pathway activation (Figure 3J). Collectively, these results demonstrate that phosphorylation at the NCL_T76 site is linked to multiple RNA regulatory pathways across diverse cancer types, underscoring the central role of RBP phosphorylation in shaping RNA regulatory networks in tumors.

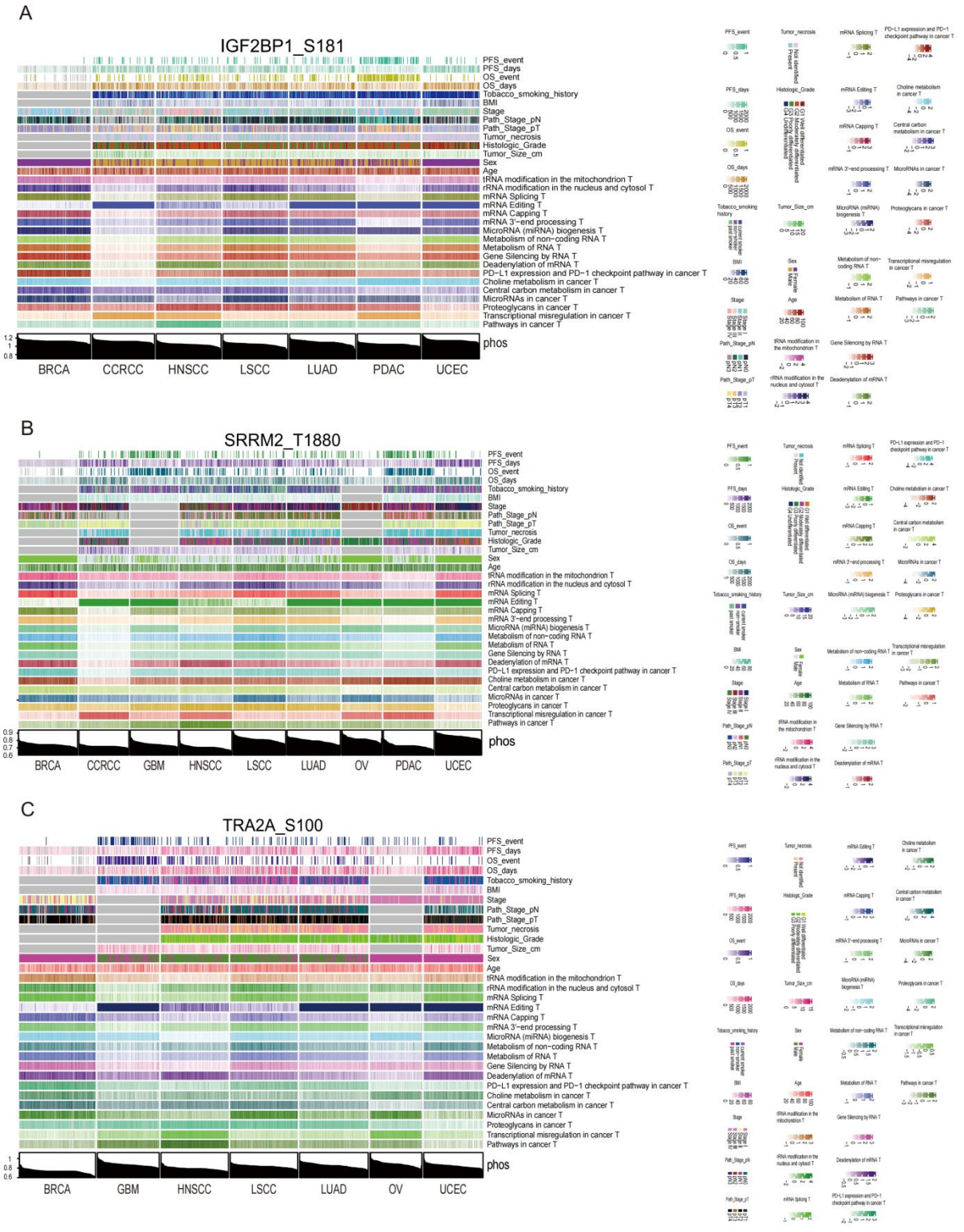

Figure 2.An pan-cancer overview of the association between known molecular and clinical features and phosphorylation of key RBPs, IGF2BP1_S181 (A), SRRM2_T1880 (B), and TRA2A_S100 (C). The bar charts showing the phosphorylation status of RBP were displayed at the bottom of the heatmap, where the samples within each cancer type were sorted by phosphorylation levels. Each row in the waterfall plot represents clinical information (e.g., age, BMI, tumor size, gender, stage) and RNA pathway enrichment scores (e.g., splicing, non-coding RNA metabolism, small RNA biogenesis) for individual patients. Categorical variables (PFS_event, OS_event, Stage, Path_Stage_pN, Path_Stage_pT, Tumor_necrosis, Histologic_Grade, Sex) are color-coded. Numerical variables (progression-free survival, overall survival, tumor size, body mass index, age, mitochondrial tRNA modification, nuclear and cytoplasmic rRNA modification, mRNA splicing, mRNA editing, mRNA capping, mRNA 3'-end processing, miRNA biosynthesis, non-coding RNA metabolism, RNA metabolism, RNA-mediated gene silencing, mRNA deadenylation) are represented by gradients of color intensity, with darker shades indicating higher values. Missing values are shown in white.

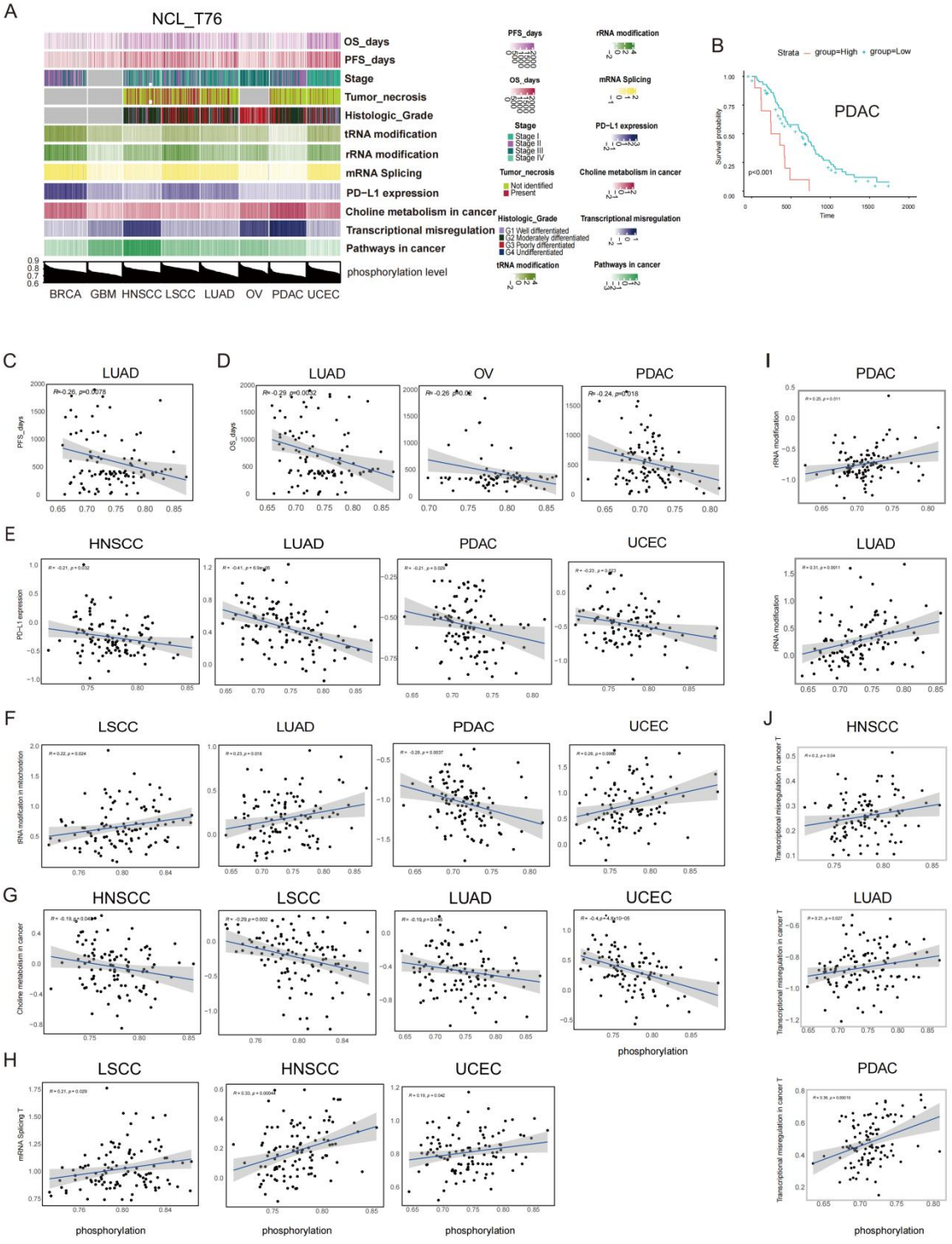

Figure 3.Differential phosphorylation of NCL T76 in pan-cancer and its correlation with clinical features and RNA function. (A) The waterfall plot of the association analysis between NCL T76 phosphorylation in pan-cancer and clinical features as well as RNA functions. (B) In PDAC, the overall survival (OS) of patients in the high NCL T76 phosphorylation group was significantly lower than that in the low phosphorylation group (log-rank test, $p < 0.001$). (C-D) Linear correlation analysis between NCL T76

phosphorylation levels and survival indicators (OS and PFS) in LUAD, OV, and PDAC. Pearson correlation analysis was applied. The gray shaded area represents the 95% confidence interval. (E-J) Pearson correlation analysis of NCL T76 phosphorylation with RNA-related and cancer-related pathways across different cancer types, including PD-1/PD-L1 expression (E), tRNA modification in the mitochondrion (F), Choline metabolism in cancer T (G), mRNA Splicing T (H), rRNA modification (I), and transcriptional dysregulation in cancer T (J).

CDK2 kinase regulates the phosphorylation of NCL_T76

To further elucidate the regulatory mechanism of NCL_T76, the 15-amino-acid sequence (TKKVAVATPAKKAAV) surrounding the NCL_T76 locus was submitted to the PhosphoSitePlus website, which predicted 303 potential kinases for this site. We considered CDK2, which had the highest site-percentile, as the most likely kinase regulating NCL_T76. Based on this result, we performed batch docking of CDK2 with small molecules using AutoDock software, yielding 84 small-molecule inhibitors. Among these, TG-02, with the highest binding energy, was selected as the CDK2 kinase inhibitor for subsequent experiments (Figure 4A-B).

Subsequently, we utilized the PANC-1 cell line (human pancreatic carcinoma), treating it with dimethyl sulfoxide (as a control) and varying concentrations of TG-02. In cellular experiments, TG-02 treatment significantly reduced the phosphorylation level of NCL_T76 (Figure 4C, right, bands 2-3), with the inhibitor treatments exhibiting a dose-dependent effect. Given that TG-02 is also known to inhibit other kinases including CDK1, CDK9, JAK2, and FLT3, this result suggests the potential involvement of CDK2 or other TG-02-sensitive kinases in regulating NCL_T76 phosphorylation. Therefore, CDK2 represents a candidate upstream kinase for NCL_T76, although direct validation using genetic approaches is required for confirmation.

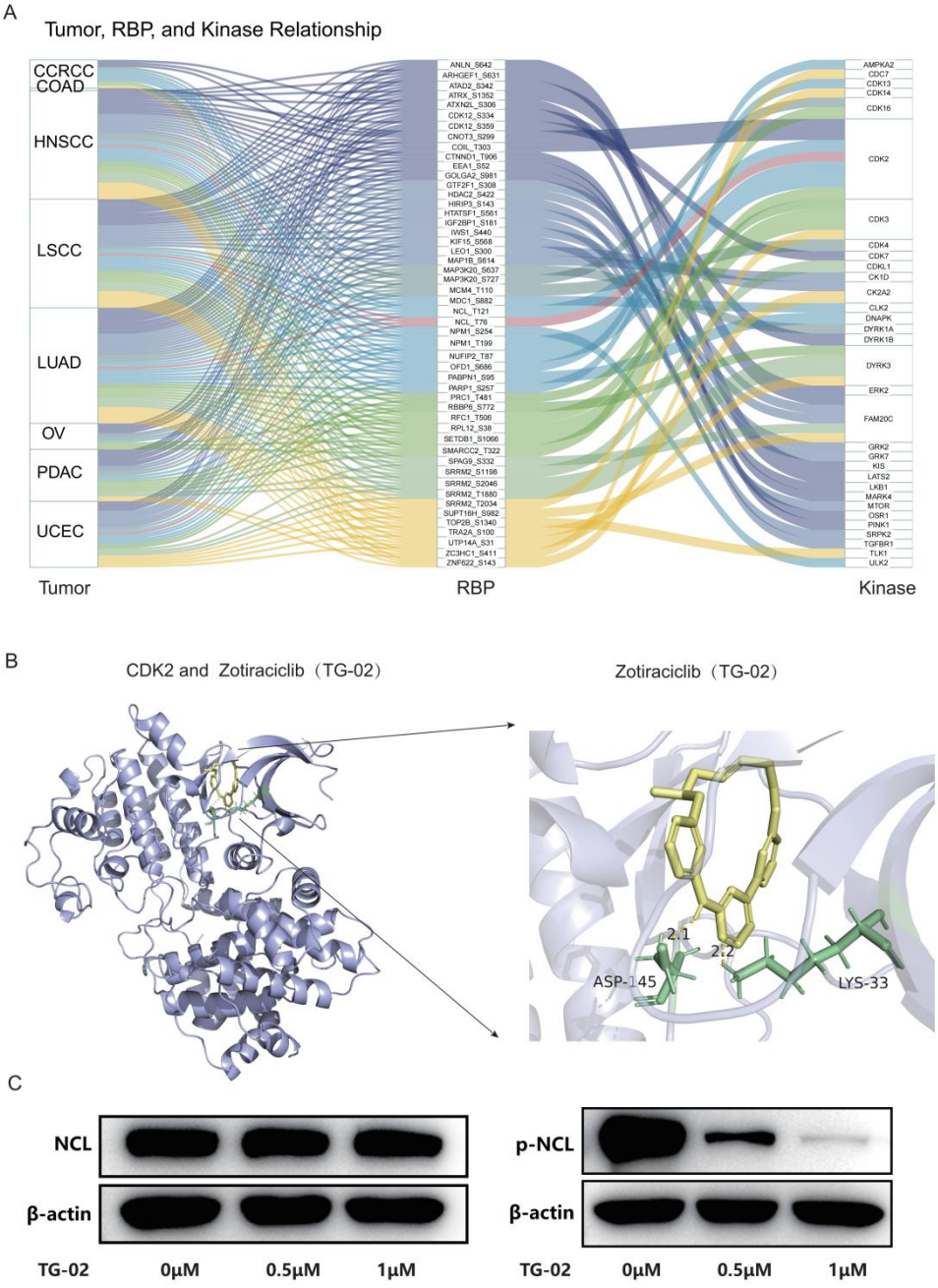

Figure 4. The regulation of targeted inhibitors on predicted kinase-mediated NCL phosphorylation. (A) A sankey diagram

illustrating 52 RBP phosphorylation gene sites and their kinases predicted from the PhosphoSitePlus database, across these 8 types of tumors. (B) Molecular docking model between the small-molecule inhibitor TG-02 (Zotiraciclib) and CDK2. A zoomed-in view of the TG-02 binding site with CDK2 shows the key hydrogen bonds and the interacting amino acid residues. (C) The Western bloting confirmed that treatment with TG-02 could inhibit the phosphorylation of NCL, using β-actin as the endogenous control. The final concentrations of TG-02 were 0.5μM and 1μM, respectively.

Discussion

In recent years, as genomic abnormalities do not fully explain cancer pathogenicity, post-transcriptional regulation has gained increasing attention for its role in cancer molecular mechanisms[15]. Moreover, in-depth studies of protein function, including phosphorylation modifications, have become an effective strategy for understanding cancer-driving mechanisms and discovering therapeutic targets[16]. RNA-binding proteins (RBPs) influence post-transcriptional regulation by modulating various processes in the RNA life cycle and are closely associated with the development and progression of cancer[17]. Previous studies have reported that phosphorylation modification serves as a critical hub connecting signal transduction with cancer phenotypes by altering the activity of RBPs, the function of RNA polymerase, and the regulatory effects of non-coding RNAs. For instance, research has demonstrated that during RNA processing, KRAS mutations induce phosphorylation of ALKBH5 at Ser325 via the ERK/JNK pathway, inhibiting its mRNA demethylation activity and leading to aberrant m^{6}A modifications in nucleotide excision repair genes, ultimately resulting in platinum resistance in lung cancer[18]. Additionally, long non-coding RNAs (lncRNAs), as key mediators of phosphorylation regulation, can modulate RNA pathways by either masking phosphorylation sites (e.g., LINP1 inhibiting eIF2α phosphorylation) or aberrantly activating kinases (e.g., CamK-A enhancing PNCK activity), thereby influencing the survival and stress responses of cancer cells. These findings collectively establish a regulatory model of "phosphorylation modification-RNA pathway-cancer phenotype," providing a theoretical basis for targeted intervention. This phosphorylation-mediated RNA pathway dysregulation is not an isolated event but forms synergistic effects with core cancer signaling networks[19]. For instance, the MYC transcription factor upregulates the expression of ribosome biogenesis-related RNAs, while phosphorylation signals from the RAS/MAPK pathway enhance its protein activity. The feedforward loop formed by these two mechanisms drives unlimited proliferation of cancer cells. However, there is currently a lack of systematic research on how phosphorylation of RBPs specifically affects RNA and biological functions[20]. In this study, we reveal the abnormal phosphorylation characteristics of RBPs in multiple cancers, innovatively and systematically analyze the regulatory relationship between RBP phosphorylation modifications and RNA, and map a landscape for further investigation of their regulatory mechanisms.

Herein, we systematically identified 52 key RBPs (those with upregulated phosphorylation in at least four cancer types) and randomly selected 4 RBPs: IGF2BP1_S181, SRRM2_T1880, TRA2A_S100, and NCL_T76, to investigate the relationship between RBP phosphorylation and cancer clinical indicators. Surprisingly, the phosphorylation of these sites was closely associated with clinical indicators and RNA regulation across various cancers. Among these, IGF2BP1, as a typical oncogenic RBP, can stabilize target mRNAs through an m^{6}A-dependent mechanism and plays a central role in solid tumors such as lung cancer. IGF2BP1 phosphorylation regulates ribonucleoprotein condensate formation by impairing low-affinity protein and RNA interactions. Clinical studies confirmed that TRA2A, as a nuclear RBP, is frequently upregulated in tumors such as liver cancer and breast cancer, promoting cell proliferation, migration, and chemotherapy resistance by altering the splicing patterns of cancer-related genes (modulating alternative splicing (AS) of precursor mRNA). It participates in the multi-process regulation of cancer and is regarded as a potential prognostic marker and therapeutic target. Its direct binding with lncRNA MALAT1 recruits EZH2 to form the PRC2 complex, thereby activating the β-catenin/Wnt signaling pathway, which is evolutionarily conserved across multiple epithelial-derived tumors.

Nucleolin (NCL), as a core factor in ribosome biogenesis, plays a pivotal role in cellular processes such as DNA and RNA metabolism, chromatin remodeling, and the cell cycle. Although existing literature has reported mechanisms of its phosphorylation-mediated RNA regulation (e.g., CK2-mediated NCL phosphorylation regulates NCL association with its target mRNA), no systematic study has yet revealed its regulatory network. In this study, the phosphorylation of Nucleolin (NCL) at the T76 site was identified as a critical functional modification, showing significant upregulation in multiple cancers and close association with poor patient prognosis. Cellular experiments revealed that the cyclin-dependent kinase CDK2 is its potential upstream kinase, and this regulatory relationship was confirmed through experiments with the small-molecule inhibitor TG-02. Although this study did not conduct an in-depth investigation into its broadly applicable molecular mechanisms across different cancers, future research will further elucidate the functions of NCL_T76 phosphorylation, combining site-directed mutagenesis and phosphorylation-specific antibodies for mechanistic studies. These findings align with our analytical conclusions, collectively demonstrating that the phosphorylation of RNA-binding proteins can indeed broadly regulate RNA, thereby modulating cellular biological functions.

CDK2 is a key kinase for the G1/S phase transition in the cell cycle, and its abnormal activation is regarded as a hallmark of cancer[21]. In ER-positive breast cancer, CDK2 phosphorylates RB protein after binding to cyclin E, thereby releasing its inhibition of the E2F transcription factor and driving cells into the proliferation cycle. In leukemia models, the high activity of CDK2 is closely associated with the maintenance of $CD34^+$ $CD38^-$ stem cell-like populations, serving as a critical factor for disease relapse[22]. TG-02, as an oral multi-target kinase inhibitor, exhibits inhibitory activity against CDK1/2/7/9, JAK2, and FLT3. Its anticancer effects stem from dual blockade of the cell cycle and transcription processes. In acute myeloid leukemia (AML), TG-02 induces G1 phase arrest by inhibiting CDK2-mediated cell cycle progression, while simultaneously reducing Ser2 phosphorylation of RNA polymerase II through CDK9 inhibition, leading to rapid degradation of short-lived anti-apoptotic proteins such as MCL1 and XIAP, ultimately activating the BAX-dependent apoptotic pathway. This dual mechanism of "cell cycle arrest + apoptosis induction" enables it to overcome cytokine-mediated survival signal protection and maintain cytotoxic activity against $CD34^+CD38^-CD123^+$

stem-like cells[23]. In vivo models demonstrated that TG-02 accumulates in tumor tissues through oral administration, significantly suppressing CDK and STAT signaling pathways and prolonging survival in AML model mice. However, its broad-spectrum anticancer activity has remained understudied, and this research represents the first attempt into its pan-cancer anticancer potential. The efficacy and resistance mechanisms of TG-02 in solid tumors, as suggested by our current computational study, may provide a preliminary theoretical foundation for future exploration.

In summary, these findings reveal the prevalence and functional significance of RBP phosphorylation in cancer, providing new evidence regarding its widespread regulation of cancer-related RNA abnormalities. These results offer novel molecular insights into dysregulated RNA in tumors and provide clues for developing precision therapeutic strategies based on phosphorylation regulation[24]. However, some limitations still exist. First, the primary data in this study were derived from the CPTAC database, which may have issues with insufficient sample representativeness. Second, experimental validation was limited to the cellular level, lacking further support from animal models and clinical samples. Third, we did not perform a detailed comparative analysis of the regulatory networks among the four identified RBP sites. Fourth, the mechanistic depth of this study is limited, as we have not elucidated how NCL_T76 phosphorylation affects RNA-binding activity or malignant cellular phenotypes. Fifth, the evidence supporting CDK2 as the upstream kinase relies solely on the multi-kinase inhibitor TG-02, lacking direct validation via genetic approaches or in vitro kinase assays. Sixth, all in vitro experiments were performed only in the PANC-1 cell line, which cannot represent a pan-cancer regulatory model. Therefore, the conclusions of this study should be considered preliminary and hypothesis-generating rather than definitive.In future studies, we should integrate multi-omics approaches, animal experiments, and clinical data to further validate the molecular mechanisms of RBP phosphorylation and its feasibility as a therapeutic target.

References

1. Méndez-Vidal, C. The p53-induced mouse zinc finger protein wig-1 binds double-stranded RNA with high affinity. Nucleic Acids Res. 30, 1991–1996 (2002). https://doi.org/10.1093/nar/30.9.1991
2. Kasowitz, S. D. et al. Nuclear m6A reader YTHDC1 regulates alternative polyadenylation and splicing during mouse oocyte development. PLoS Genet. 14, e1007412 (2018). https://doi.org/10.1371/journal.pgen.1007412
3. Guo, L. & Shorter, J. Biology and Pathobiology of TDP-43 and Emergent Therapeutic Strategies. Cold Spring Harb. Perspect. Med. 7, a024554 (2016). https://doi.org/10.1101/cshperspect.a024554
4. Fabbiano, F. et al. RNA packaging into extracellular vesicles: An orchestra of RNA-binding proteins? J. Extracell. Vesicles 10, e12043 (2020). https://doi.org/10.1002/jev2.12043
5. Hossain, F. et al. Notch Signaling Regulates Mitochondrial Metabolism and NF-κB Activity in Triple-Negative Breast Cancer Cells via IKKα-Dependent Non-canonical Pathways. Front. Oncol. 8, 575 (2018). https://doi.org/10.3389/fonc.2018. 00575
6. Kandoth, C. et al. Mutational landscape and significance across 12 major cancer types. Nature 502, 333–339 (2013). https://doi.org/10.1038/nature12634
7. Yang, W. et al. PKM2 Phosphorylates Histone H3 and Promotes Gene Transcription and Tumorigenesis. Cell 150, 685–696 (2012). https://doi.org/10.1016/j.cell.2012.07.018
8. Wang, Y. et al. Epigenetic modification of m6A regulator proteins in cancer. Mol. Cancer 22, 102 (2023). https://doi.org/ 10.1186/s12943-023-01805-y
9. Qin, H. et al. RNA-binding proteins in tumor progression. J. Hematol. Oncol. 13, 90 (2020). https://doi.org/10.1186/s13045-020- 00927-w
10. Statello, L. et al. Gene regulation by long non-coding RNAs and its biological functions. Nat. Rev. Mol. Cell Biol. 22, 96–118 (2020). https://doi.org/10.1038/s41580-020-00315-9
11. Tripathi, V. et al. Long Noncoding RNA MALAT1 Controls Cell Cycle Progression by Regulating the Expression of Oncogenic Transcription Factor B-MYB. PLoS Genet. 9, e1003368 (2013). https://doi.org/10.1371/journal.pgen.1003368
12. Hunter, T. Oncoprotein Networks. Cell 88, 333–346 (1997). https://doi.org/10.1016/s0092-8674(00)81872-3
13. Naro, C. & Sette, C. Phosphorylation-Mediated Regulation of Alternative Splicing in Cancer. Int. J. Cell Biol. 2013, 1–15 (2013). https://doi.org/10.1155/2013/985394
14. Kang, D. et al. Inhibition of Specificity Protein 1 Is Involved in Phloretin-Induced Suppression of Prostate Cancer. BioMed Res. Int. 2020, 1358674 (2020). https://doi.org/10.1155/2020/1358674
15. Wong, C.-M. et al. Non-coding RNAs in hepatocellular carcinoma: molecular functions and pathological implications. Nat. Rev. Gastroenterol. Hepatol. 15, 137–151 (2018). https://doi.org/10.1038/nrgastro.2017.169
16. Shu, F. et al. Epigenetic and post-translational modifications in autophagy: biological functions and therapeutic targets. Signal Transduct. Target. Ther. 8, 32 (2023). https://doi.org/10.1038/s41392-022-01300-y
17. Yang, Y. et al. O-GlcNAcylation of YTHDF2 promotes HBV-related hepatocellular carcinoma progression in an N6-methyladenosine-dependent manner. Signal Transduct. Target. Ther. 8, 63 (2023). https://doi.org/10.1038/s41392-023-01324-y
18. Yu, M. et al. The role of m6A demethylases in lung cancer: diagnostic and therapeutic implications. Front. Immunol. 14, 1279735 (2023). https://doi.org/10.3389/fimmu.2023.1279735

19. Shapiro, G. I. Cyclin-Dependent Kinase Pathways As Targets for Cancer Treatment. J. Clin. Oncol. 24, 1770–1783 (2006). https://doi.org/10.1200/jco.2005.03.7689
20. Sugiura, R. et al. Role of RNA-Binding Proteins in MAPK Signal Transduction Pathway. J. Signal Transduct. 2011, 1–8 (2011). https://doi.org/10.1155/2011/921473
21. Geng, J. et al. Abstract 5705: Discovery of a selective slow-off CDK2 inhibitor NKT3447 with distinct features of suppressing pCDK2, downregulating cyclin E, and achieving prolonged pathway inhibition. Cancer Res. 84, 5705 (2024). https://doi.org/10.1158/1538-7445.am2024-5705
22. Goh, K. C. et al. TG02, a novel oral multi-kinase inhibitor of CDKs, JAK2 and FLT3 with potent anti-leukemic properties. Leukemia 26, 236–243 (2011). https://doi.org/10.1038/leu.2011. 284
23. Jin, Y. et al. Recent Development of CDK2 Inhibitors as Anticancer Drugs: An Update (2015–2023). Pharm. Front. 06, e195–e220 (2024). https://doi.org/10.1055/s-0044-1788286
24. An, S. et al. Integrative network analysis identifies cell-specific trans regulators of m6A. Nucleic Acids Res. 48, 1715–1729 (2020). https://doi.org/10.1093/nar/gkz1206

Author Contributions

All authors made significant contributions to this study. Ziyi Liu was responsible for data collection and analysis, as well as manuscript drafting and initial writing. Jinwan Li performed experimental validation. Ping Cui carried out critical revision and final approval of the manuscript. Sanqi An designed the research concept. Jing Leng developed the experimental protocols. All authors have reviewed and approved the final version of the manuscript.

Funding Statement

This study did not receive any specific funding from any grant agency, funding body, or public/private sector.

Ethics Statement

This study did not involve human subjects or animal experiments. All experiments were conducted using commercially available cell lines and followed standard laboratory operating procedures.

Consent for Publication

All authors have read and approved the final version of the manuscript and consent to its publication in iCell. There is no dispute regarding any third-party copyright or ownership rights related to this manuscript.

Data and Code Availability Statement

The data supporting the findings of this study were obtained from the LinkedOmics database (http://www.linkedomics.org), which integrates multi-omics data from The Cancer Genome Atlas (TCGA) and the Clinical Proteomic Tumor Analysis Consortium (CPTAC). No new data were generated in this study.